Discover Oncology

Research

Differential expression of capecitabine-related metabolic enzymes in hepatocellular carcinoma and its clinical value: a retrospective cohort study

Jianing Lu[1] · Zhiqi Yin[2] · Yan Zhuang[7] · Zhenglu Wang[3,4,5] · Hong Zheng[4,5] · Lei Cao[3] · Dejun Kong[6] · Jinliang Duan[6] · Shaofeng Chen[6] · Tao Chen[6]

Received: 5 April 2025 / Accepted: 23 May 2025
Published online: 12 June 2025

Abstract

Background Capecitabine (CAP) is widely used in cancer treatment for its oral convenience and tumor targeting. However, its effectiveness in hepatocellular carcinoma (HCC) is suboptimal, possibly due to metabolic enzyme expression differences. This study aims to analyze these enzymes' expression differences and explore their correlation with clinical pathological factors, to inform personalized CAP treatment.

Methods This retrospective study used Immunohistochemistry (IHC) to analyze tumor and non-tumorous samples from HCC patients for CAP metabolic enzyme expression. PRM protein quantification was performed on 10% of samples to validate IHC results. Clinical and pathological data were collected, and multivariable linear regression was used to identify independent risk factors.

Results This study analyzed 60 HCC patients with hepatitis B and cirrhosis, revealing significant differences in CAP metabolic enzymes expression between tumor and non-tumorous tissues, with greater individual differences in tumors. Cytidine deaminase (CDA) levels in tumors decreased as liver function deteriorated ($P = 0.023$), while thymidine phosphorylase (TP) levels increased ($P < 0.001$). Tumor tissue had lower levels of carboxylesterase 1–2 (CES1-2), CDA, and dihydropyrimidine dehydrogenase (DPYD) but higher TP levels than non-tumorous and normal liver tissues. In tumor tissue, CDA (CV: 118.70%, SD: 3.897) and CES2 (CV: 94.90%, SD: 2.910) showed the greatest individual variability. Multivariable linear regression identified independent risk factors affecting CAP metabolic enzyme expression.

Conclusion This study has found significant variability in the expression of CAP metabolic enzymes across individuals and tissues. Developing a treatment flowchart based on metabolic enzymes provides a foundation for personalized HCC treatment and enhances the effectiveness of CAP therapy.

Jianing Lu and Zhiqi Yin have contributed equally as the first authors of this work.

Supplementary Information The online version contains supplementary material available at https://doi.org/10.1007/s12672-025-02807-6.

✉ Zhenglu Wang, 13920474643@163.com; ✉ Hong Zheng, zhenghongyx@139.com | [1]The First Central Clinical College, Tianjin Medical University, No. 24 Fukang Road, Nankai District, Tianjin 300070, China. [2]Department of Pathology, Tianjin First Central Hospital, First Central Clinical College, Tianjin Medical University, No. 24 Fukang Road, Nankai District, Tianjin 300192, China. [3]The Biospecimen Resource Sharing Center, Tianjin First Central Hospital, First Central Clinical College, Tianjin Medical University, No. 24 Fukang Road, Nankai District, Tianjin 300192, China. [4]Organ Transplant Department, Tianjin First Central Hospital, First Central Clinical College, Tianjin Medical University, No. 24 Fukang Road, Nankai District, Tianjin 300192, China. [5]Key Laboratory of Transplant Medicine, Chinese Academy of Medical Sciences, First Central Clinical College, Tianjin Medical University, Tianjin 300192, China. [6]School of Medicine, Nankai University, No. 94, Weijin Road, Nankai District, Tianjin 300071, China. [7]Department of Health Service, Military Health Education Section, Logistics College of People's Armed Police Force, No. 1 Hui Zhi Huan Road, Dong Li District, Tianjin 300309, China.

Clinical Trial Number: Not applicable.

Keywords Capecitabine · Metabolic enzymes · Hepatocellular carcinoma · Individual variability · Clinical pathological correlation

1 Introduction

Capecitabine (CAP) is an oral prodrug of 5-fluorouracil (5-FU) and serves as a first-line therapeutic for various cancers, including colorectal, breast, and gastric cancers. This is due to its oral convenience, tumor targeting, and minimal toxicity to healthy tissues [1]. The metabolic conversion of CAP within the body is pivotal for its pharmacological characteristics, involving the synergistic action of several metabolic enzymes. As shown in Fig. 1, most of CAP's metabolic activation occurs in the liver, following a strict cascade reaction. In this reaction, carboxylesterase (CES), cytidine deaminase (CDA), and thymidine phosphorylase (TP) sequentially function to ultimately transform CAP into the active drug component 5-FU, with the final degradation of 5-FU being achieved by dihydropyrimidine dehydrogenase (DPYD) [2]. Recent studies have shown that the liver expresses CES1 and its isoenzyme CES2, contributing to CAP metabolism [3]. Moreover, TP levels in tumor cells are 3–10 times higher than in normal cells and are also present in normal hepatocytes. This underpins CAP's tumor-targeting and potential for liver damage [4]. DPYD, the rate-limiting enzyme in fluorouracil catabolism, is widely expressed in various tumors and normal tissues, with particularly high levels in the liver [5].

Current research indicates that although CAP metabolic enzymes are present in liver tissue, CAP's efficacy in treating hepatocellular carcinoma (HCC) is less pronounced than in other cancers [6, 7]. Only some studies have shown significant efficacy of CAP in advanced HCC, it is not a first-line treatment for HCC in clinical practice [8]. This suggests that other factors may influence the effectiveness of CAP in HCC treatment. Unlike patients with other cancers, most HCC patients have underlying liver conditions. This may alter the expression of CAP metabolic enzymes, impacting drug efficacy and contributing to its suboptimal performance in HCC treatment. CAP metabolic enzyme expression may also show individual and tissue variations, leading to differences in CAP efficacy among HCC patients. Although some studies have shown that the ratio of TP to DPYD expression is positively correlated with CAP efficacy [9], research viewing the CAP metabolic process as an overall cascade reaction is lacking, especially regarding individual and tissue differences in the expression of upstream metabolic enzymes like CES and CDA, and their correlation with clinical pathology. Thus, studies focusing on personalized application strategies for CAP and the development of novel molecular targeted agents for HCC are urgently needed and of great importance [10].

This study aims to assess the individual and tissue differences of CAP metabolic enzymes in HCC patients with underlying liver disease by analyzing the expression levels of these enzymes in HCC tissue, non-tumorous tissue, and normal liver tissue. The study also seeks to identify risk factors affecting CAP metabolic enzyme expression in HCC tissue. These findings will provide theoretical support for the personalized application of CAP in HCC patients, potentially improving CAP efficacy and optimizing HCC treatment.

2 Materials and methods

This retrospective cohort study was conducted by the Declaration of Helsinki and STROCSS 2021 guidelines [11], with ethical approval granted by the Clinical Research Ethics Committee of Tianjin Medical University First Central Hospital (Approval ID: STEC-TFCH-2023-HM-2). Written informed consent was obtained from all participants or legal guardians before enrollment, authorizing the use of clinical data and pathological specimens for research. Donor livers were exclusively procured from brain-deceased individuals under stringent eligibility criteria, excluding high-risk donors (infection/tumor transmission risk > 10%) as per Disease Transmission Advisory Board protocols. All organs were procured in-house following family consent and legal documentation, with allocation managed through the Chinese Organ Transplant Response System. No organs originated from prisoners.

2.1 Study design and data collection

This retrospective cohort study analyzed fresh-frozen specimens from HCC patients with hepatitis B and cirrhosis undergoing liver transplantation at Tianjin Medical University First Central Hospital Biobank (January 2019–May 2024). Samples

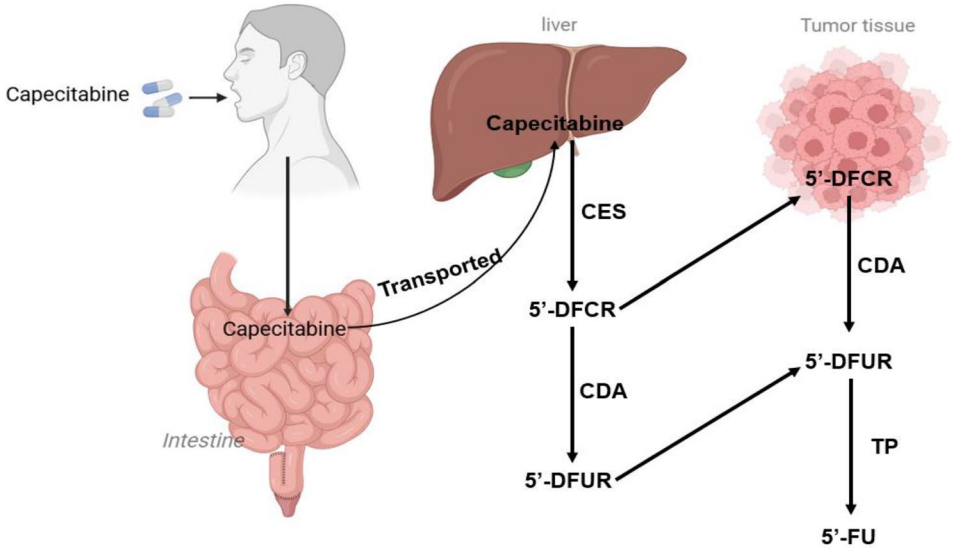

Fig. 1 Capecitabine Metabolic Pathway Diagram (CES, carboxylesterase; CDA, cytidine deaminase; TP, thymidine phosphorylase; 5′-DFCR, 5′-Deoxy-5-fluorocytidine; 5′-DFUR, 5′-Deoxy-5-fluorouridine; 5′-FU, 5′-Fluorouracil)

comprised paired tumor/non-tumor tissues and a 10% subset of normal donor liver tissues as controls. Inclusion criteria included: (i) age ≥ 18 years; (ii) pathologically confirmed HCC; (iii) complete clinicopathological records (liver function, tumor markers, staging, grading); (iv) informed consent for sample/data usage. Exclusion criteria were: (i) prior antitumor therapies(e.g., chemotherapy); (ii) > 30% necrosis in tumor/non-tumor tissues. Participants were stratified into Child–Pugh classes A, B, and C. CAP metabolizing enzyme(CES1, CES2, CDA, TP, DPYD) expression was quantitatively assessed by immunohistochemistry (IHC) staining indices. A randomly selected 10% samples were analyzed by liquid chromatography-mass spectrometry (LC–MS) based parallel reaction monitoring (PRM) to quantify CAP metabolizing enzyme and validate IHC staining results. Relative protein abundance was used as the quantitative measure. IHC staining index accuracy was confirmed by IHC-PRM concordance analysis.

Data collection encompassed three domains: (1) Demographics (age, gender); (2) Pathological characteristics (histological grade, tumor number/maximum diameter, portal vein thrombosis, IHC markers: heat shock protein 70 [HSP70], thymidylate synthase [TS], Ki-67, tumor protein p53 [P53], alpha-fetoprotein [AFP]); and (3) Clinical parameters (performance status score [PS Score], China liver cancer staging, [CNLC], Child–Pugh score and grade, Child–Pugh staging, tumor T staging, albumin, alanine aminotransferase [ALT], aspartate transaminase [AST], direct bilirubin [DBIL], total bilirubin [TBIL], indirect bilirubin [IBIL], plasma AFP, hydroperitoneum, prothrombin time). The primary outcome was the CAP-metabolizing enzyme IHC staining index, with secondary outcomes identifying risk factors for enzyme expression variability in HCC tissues.

2.2 Immunohistochemistry (IHC) analysis

To determine the expression levels of CAP metabolic enzymes in HCC tissue, non-tumorous tissue, and normal liver tissue, this study conducted an immunohistochemistry (IHC) detection analysis. First, paraffin-embedded pathological tissue sections were deparaffinized in xylene three times, each lasting 10 min. Following dewaxing through a graded ethanol series (absolute, 95%, 85%, 75%), tissues underwent triple-distilled H2O rinses. HIER (Heat-Induced Epitope Retrieval) was performed using Tris–EDTA buffer (pH 8.0) at 98 °C (40 min), followed by 3% H_2O_2-mediated peroxidase blockade (10 min). Post-fixation with paraformaldehyde (4 µm sections), slides were immunostained with the following: CES1/CES2 (1:500, 16912/15378, Proteintech), CDA (1:2000, ab222515; Abcam), TP (1:100, 12383-1-AP, Proteintech), and DPYD (1:500, 27662-1-AP, Proteintech) [7]. The antibodies used were validated by the manufacturer to specifically recognize the corresponding CAP metabolic enzymes without cross-reactivity. Antibody concentrations were optimized by preliminary experiments and referenced to the manufacturer's recommendations to ensure specific staining and minimal background interference. Subsequently, sections were treated with HRP-conjugated secondary antibodies and developed using a chromogenic substrate (DAB), followed by hematoxylin counterstaining. Tissues were then dehydrated through an ethanol gradient and permanently mounted with a resinous medium.

The IHC staining index was computed by multiplying two parameters: (1) staining intensity (0: none; 1: weak; 2: moderate; 3: strong brown signal) and (2) positively stained area (1: 0–25%; 2: 26–50%; 3: 51–75%; 4: 76–100% of tissue section)

[12]. Two pathologists independently scored five random ×40 fields of each tissue sample and calculated the staining index separately to ensure the objectivity and consistency of the scoring. The entire quantitative experimental process was conducted under blinded conditions to ensure the accuracy and reproducibility of the results.

2.3 Quantification of CAP metabolic enzymes by PRM-LC–MS

In this study, PRM-LC-MS was utilized to validate the expression levels of CAP metabolic enzymes. Exploit the correlation between the relative protein abundance quantified by PRM and the IHC staining index to evaluate the precision of the IHC staining index.

2.3.1 Protein extraction

Frozen specimens (− 80 °C) were cryogenically pulverized in liquid nitrogen-chilled mortars. The resultant powder was homogenized in 4× volume lysis buffer (1% Triton X-100, 1% protease inhibitor cocktail) with ultrasonic disruption. Subsequent phenol–chloroform extraction (1:1 v/v Tris-equilibrated phenol) was performed, followed by centrifugation (5,500×*g*, 10 min, 4 °C). The aqueous phase was precipitated overnight at − 20 °C with 5 volumes of 0.1 M ammonium acetate/methanol (5:1). Pellets were sequentially washed with methanol-acetone (1:1) and air-dried, followed by solubilization in 8 M urea. Protein quantification was conducted using a commercial BCA assay kit (Vazyme Biotech, China).

2.3.2 Enzymatic digestion

Identical protein aliquots were subjected to trypsinization. After volume normalization with lysis buffer, proteins were acid-precipitated by dropwise addition of 20% TCA (v/v) under vortex-mixing, followed by 2-h incubation at 4 °C. Following centrifugation (4,500×*g*, 5 min, 4 °C), pellets were washed thrice with ice-cold acetone and air-dried. Protein pellets were solubilized in 200 mm triethylammonium bicarbonate (TEAB) and ultrasonicated (30 s pulses, 50% amplitude). Trypsin (1:50 w/w enzyme: substrate ratio) was introduced for 16-h digestion at 37 °C. Subsequent reduction (5 mM DTT, 56 °C, 30 min) and alkylation (11 mm IAA, dark, RT, 15 min) steps completed cysteine modification.

2.3.3 LC–MS/MS analysis

Peptides were dissolved in mobile phase A, consisting of 0.1% formic acid and 2% acetonitrile in aqueous solution, and separated via an EASY-nLC1200 ultra-high performance liquid chromatography (UHPLC) system. The mobile phase composition included solvent A (0.1% formic acid, 2% acetonitrile) and solvent B (0.1% formic acid, 90% acetonitrile). Chromatographic separation employed a 30-min linear gradient programmed as follows: from 0 to 16 min, solvent B increased from 7 to 23%; between 16 and 22 min, it further rose to 35%; from 22 to 26 min, it escalated to 80%, followed by an isocratic phase at 80% B until 30 min. The flow rate remained constant at 500 nL/min throughout the process.

Following chromatographic separation via the UHPLC system, peptides were ionized through an NSI source and analyzed on an Orbitrap Exploris 480 mass spectrometer. Instrument parameters included an ion spray voltage of 2,100 V, with precursor and product ions analyzed in the high-resolution Orbitrap detector. Full MS scans (500–800 m/z) were acquired at 60,000 resolution, while MS/MS scans utilized 15,000 resolution. Data-independent acquisition (DIA) was implemented with 27% higher-energy collisional dissociation (HCD) collision energy. Operational settings were configured as follows: primary MS AGC target 300% with 50 ms maximum injection time; secondary MS AGC 100% with 220 ms injection time and 1.6 m/z isolation window.

2.3.4 Data analysis

Mass spectrometry data were analyzed in Skyline 21.1 with the following configurations: Proteolytic digestion parameters included trypsin (cleavage at KR/P termini) with zero missed cleavages allowed, peptide length restricted to 7–25 residues, and cysteine carbamidomethylation as a fixed modification. Transition settings specified precursor ions with +2/+3 charges and product ions with +1 charge, monitoring b/y-type fragments. Fragment ion selection spanned the third to terminal ions, with a mass accuracy threshold of 0.02 Da for spectral matching.

2.4 Statistical analysis

This study aims to compare the expression of CAP metabolic enzymes between HCC tissue and non-tumorous tissue. Anticipating a normal distribution, with an effect size of 0.5, a significance level of 0.05, and a desired statistical power of 0.80, Gpower software (version 3.1.9.2) was utilized to determine that a minimum of 51 samples per group is necessary. Considering a 10% dropout rate, the study enrolled a total of 60 HCC patients, yielding 120 samples in total. This study employs R software (4.2.2) and GraphPad Prism (9.0) for statistical analysis. After testing for normality and homogeneity of variance, parametric or non-parametric tests were applied, with all tests being two-tailed.

Normally distributed continuous variables were expressed as mean ± SD and analyzed via Student's t-test. Nonparametric continuous data were reported as median (IQR) with Mann–Whitney U test comparisons. Categorical variables were presented as frequency percentages and assessed via χ^2 test or Fisher's exact test, where applicable. Pearson's correlation coefficient is used to assess the correlation between PRM quantification and the IHC staining index. To identify risk factors influencing the expression of CAP metabolic enzymes in HCC tissue, the study employs univariate and multivariate linear regression analyses. To control for collinearity and follow the Events per Variable (EPV) principle, variables are preliminarily screened via LASSO regression. Should LASSO analysis fail to identify any variables, all variables are included in the multivariate analysis [13]. A *P*-value of less than 0.050 is considered to indicate statistical significance.

3 Result

3.1 Patient clinicopathological characteristics

This study analyzed 60 HCC cases and 6 donor livers (January 2019–May 2024), stratified into Child–Pugh classes A (n = 17), B (n = 21), and C (n = 22). Demographics are summarized in Table 1, with a mean age of 54 ± 7 years and a balanced gender distribution (male: 60.0%; female: 40.0%). No significant intergroup differences in age or gender were observed (age: $P = 0.112$; gender: $P = 0.715$). Clinical parameters (excluding IBIL) and pathological features (histological grade, tumor size, Ki-67, AFP IHC) significantly differed across Child–Pugh classes ($P < 0.05$), reflecting tumor biological variations under distinct hepatic functional states.

3.2 Correlation of CAP metabolic enzyme expression with hepatic function status

Figure 2 and Table 1 depict CAP-metabolizing enzyme expression stratified by liver function. In tumor tissues, CES1 and DPYD expression showed no association with liver functional status ($P > 0.05$). CDA levels were significantly higher in Child–Pugh A versus C tumors ($P = 0.023$), suggesting progressive CDA downregulation with worsening liver function. TP expression inversely correlated with liver function, being markedly lower in Child–Pugh A than B ($P = 0.033$) and C ($P < 0.001$). In non-tumorous tissues, only CES1 differed significantly between Child–Pugh B and C ($P = 0.048$), while other enzymes remained unaffected by functional decline.

3.3 Expression variability of CAP metabolic enzymes across tissue types and individual variability

Figure 3 and Table 2 show tissue-specific expression of CAP-metabolizing enzymes. Tumor tissues had lower CES1 than non-tumorous tissues ($P = 0.033$) but were similar to normal liver tissues ($P = 0.336$). CES2 decreased progressively from normal to non-tumorous to tumor tissues (tumor vs. non-tumorous, $P < 0.001$; tumor vs. normal, $P < 0.001$; non-tumorous vs normal, $P < 0.001$). CDA expression was significantly lower in tumor tissue compared with non-tumorous tissue ($P < 0.001$) and normal tissue ($P = 0.005$), while no significant difference was observed between non-tumorous and normal tissues ($P = 0.296$). Conversely, TP was upregulated in tumors compared to both non-tumorous ($P < 0.001$) and normal tissues ($P = 0.011$), with no difference between non-tumorous and normal tissues ($P = 0.915$). DPYD expression was reduced in tumor tissue compared with non-tumorous tissue ($P < 0.001$) and normal tissue ($P = 0.018$), while no significant difference was observed between non-tumorous and normal tissues ($P = 0.471$).

Table 2 delineates the interindividual variability of CAP-metabolizing enzymes across tissues. Normal liver tissues exhibited zero coefficient of variation (CV) and standard deviation (SD) for all enzymes, indicating the absence of interindividual variability. In tumor tissues, all enzymes demonstrated marked variability, with CDA (CV: 118.70%; SD: 3.897)

Table 1 Patient demographics and baseline characteristics

Characteristic	Total (n = 60[a])	Child–Pugh classification			*P* value[b]
		Child–Pugh A (n = 17[a])	Child–Pugh B (n = 21[a])	Child–Pugh C (n = 22[a])	
Age (years)	54 ± 7	54 ± 7	56 ± 7	51 ± 7	0.112
Gender					0.715
Female	24 (40.0%)	7 (41.2%)	7 (33.3%)	10 (45.5%)	
Male	36 (60.0%)	10 (58.8%)	14 (66.7%)	12 (54.5%)	
CES1(T^c)	12.00 (12.00, 12.00)	12.00 (12.00, 12.00)	12.00 (12.00, 12.00)	12.00 (12.00, 12.00)	0.826
CES1(NT^d)	12.00 (12.00, 12.00)	12.00 (12.00, 12.00)	12.00 (12.00, 12.00)	12.00 (12.00, 12.00)	0.026
CES2(T^c)	2.00 (0.00, 4.50)	2.00 (0.00, 4.00)	2.00 (1.00, 4.00)	3.50 (1.25, 6.00)	0.235
CES2(NT^d)	6.0 (4.0, 8.0)	6.0 (4.0, 8.0)	6.0 (4.0, 8.0)	7.0 (4.0, 8.0)	0.955
CDA(T^c)	2.0 (0.0, 6.0)	3.0 (2.0, 8.0)	0.0 (0.0, 8.0)	1.0 (0.0, 2.0)	0.177
CDA(NT^d)	9.00 (8.00, 12.00)	9.00 (8.00, 12.00)	9.00 (8.00, 12.00)	8.50 (8.00, 11.25)	0.621
TP(T^c)	9.0 (6.0, 12.0)	6.0 (2.0, 8.0)	9.0 (6.0, 12.0)	11.0 (9.0, 12.0)	< 0.001
TP(NT^d)	3.00 (2.00, 6.00)	3.00 (2.00, 6.00)	3.00 (2.00, 4.00)	4.00 (3.00, 6.00)	0.113
DPYD(T^c)	9.00 (8.00, 12.00)	9.00 (8.00, 12.00)	9.00 (8.00, 12.00)	9.00 (8.25, 9.00)	0.842
DPYD(NT^d)	12.00 (12.00, 12.00)	12.00 (12.00, 12.00)	12.00 (12.00, 12.00)	12.00 (12.00, 12.00)	0.126
Histological grading					0.047
Grade III	35 (58.3%)	9 (52.9%)	9 (42.9%)	17 (77.3%)	
Grade II	18 (30.0%)	7 (41.2%)	8 (38.1%)	3 (13.6%)	
Grade IV	6 (10.0%)	0 (0.0%)	4 (19.0%)	2 (9.1%)	
Grade I	1 (1.7%)	1 (5.9%)	0 (0.0%)	0 (0.0%)	
No. of tumors	2.00 (1.00, 3.00)	1.00 (1.00, 2.00)	2.00 (1.00, 3.00)	2.50 (1.00, 3.00)	0.114
Maximum tumor diameter (cm)	5.75 (3.00, 7.50)	3.00 (2.00, 5.00)	6.50 (4.50, 8.00)	6.20 (5.05, 7.50)	0.002
Portal vein tumor thrombosis					0.124
No	47 (78.3%)	15 (88.2%)	18 (85.7%)	14 (63.6%)	
Yes	13 (21.7%)	2 (11.8%)	3 (14.3%)	8 (36.4%)	
Ki-67	0.50 (0.22, 0.70)	0.20 (0.15, 0.30)	0.45 (0.35, 0.65)	0.70 (0.60, 0.75)	< 0.001
HSP70					0.223
Negatives	12 (20.0%)	6 (35.3%)	3 (14.3%)	3 (13.6%)	
Positive	48 (80.0%)	11 (64.7%)	18 (85.7%)	19 (86.4%)	
TS					0.439
Negatives	22 (36.7%)	8 (47.1%)	8 (38.1%)	6 (27.3%)	
Positive	38 (63.3%)	9 (52.9%)	13 (61.9%)	16 (72.7%)	
P53					0.886
Negatives	35 (58.3%)	10 (58.8%)	13 (61.9%)	12 (54.5%)	
Positive	25 (41.7%)	7 (41.2%)	8 (38.1%)	10 (45.5%)	
AFP(IHC)					< 0.001
Negatives	30 (50.0%)	16 (94.1%)	13 (61.9%)	1 (4.5%)	
Positive	30 (50.0%)	1 (5.9%)	8 (38.1%)	21 (95.5%)	
CNLC staging					< 0.001
Grade I	15 (25.0%)	11 (64.7%)	4 (19.0%)	0 (0.0%)	
Grade II	16 (26.7%)	4 (23.5%)	7 (33.3%)	5 (22.7%)	
Grade III	12 (20.0%)	2 (11.8%)	4 (19.0%)	6 (27.3%)	
Grade IV	17 (28.3%)	0 (0.0%)	6 (28.6%)	11 (50.0%)	
T staging					< 0.001
T1	12 (20.0%)	8 (47.1%)	1 (4.8%)	3 (13.6%)	
T2	13 (21.7%)	5 (29.4%)	7 (33.3%)	1 (4.5%)	
T3	27 (45.0%)	4 (23.5%)	12 (57.1%)	11 (50.0%)	
T4	8 (13.3%)	0 (0.0%)	1 (4.8%)	7 (31.8%)	
PS score	2.00 (2.00, 3.00)	2.00 (1.00, 2.00)	2.00 (2.00, 3.00)	2.50 (2.00, 3.00)	< 0.001

Table 1 (continued)

Characteristic	Total (n = 60[a])	Child–Pugh classification			*P* value[b]
		Child–Pugh A (n = 17[a])	Child–Pugh B (n = 21[a])	Child–Pugh C (n = 22[a])	
Child–Pugh score	8.50 (6.00, 11.00)	5.00 (5.00, 6.00)	8.00 (7.00, 9.00)	12.00 (11.00, 12.00)	< 0.001
Albumin (g/L)	34 ± 7	40 ± 4	33 ± 7	29 ± 5	< 0.001
ALT(μ/L)	63 (35, 224)	25 (18, 39)	85 (40, 212)	221 (153, 278)	< 0.001
AST(μ/L)	50 (35, 114)	38 (31, 46)	47 (34, 91)	95 (50, 146)	< 0.001
DBIL(μ/L)	33 (10, 75)	10 (5, 12)	36 (13, 74)	63 (33, 111)	< 0.001
TBIL(μ/L)	38 (23, 95)	21 (15, 24)	38 (25, 62)	92 (43, 124)	< 0.001
IBIL(μ/L)	15 (10, 33)	12 (9, 14)	15 (10, 33)	30 (13, 34)	0.157
AFP (plasma) (ng/ml)	472 (33, 696)	23 (7, 64)	463 (73, 661)	704 (539, 2,236)	< 0.001
Hydroperitoneum					0.006
Negatives	44 (73.3%)	17 (100.0%)	13 (61.9%)	14 (63.6%)	
Positive	16 (26.7%)	0 (0.0%)	8 (38.1%)	8 (36.4%)	
Prothrombin time	15.70 (12.40, 18.13)	12.30 (11.50, 13.20)	16.40 (13.30, 17.10)	18.15 (15.80, 19.10)	< 0.001

[a]Mean ± SD; n (%); Median (IQR)

[b]One-way ANOVA; Pearson's Chi-squared test; Kruskal–Wallis rank sum test; Fisher's exact test

[c]T: IHC staining index in Tumor tissues

[d]NT: IHC staining index in Non-Tumor tissues

and CES2 (CV: 94.90%; SD: 2.910) displaying the highest variability. In non-tumorous tissues, TP exhibited moderate variability (CV: 68.23%; SD: 2.650), while other enzymes showed lower variability compared to tumor tissues. These findings suggest that tumorigenesis may reduce TP expression heterogeneity while amplifying variability in other enzymes.

3.4 Correlation analysis of CAP metabolic enzyme IHC staining index and PRM protein quantification

Figure 4 presents the correlation analysis outcomes between the IHC staining index of CAP metabolic enzymes and PRM protein quantification. In tumor tissue, the IHC staining index of each enzyme all exhibited a strong correlation with the PRM quantification results, with Pearson's correlation coefficients (r) of 0.9443 (CES1), 0.8913 (CES2), 0.9934 (CDA), 0.9975 (TP), and 0.8285 (DPYD), and *P*-values of 0.0046, 0.0171, < 0.0001, < 0.0001, and 0.0416, respectively. Notably, the correlation coefficient for DPYD detection by the two methods indicated a strong positive correlation ($r > 0.7$), but the *P* value of 0.0416, approaching the significance threshold ($P < 0.05$). In non-tumorous tissue, the IHC staining index also showed a strong correlation with the PRM quantification results. Specifically, the Pearson's correlation coefficients (r) were 0.8826 (CES1), 0.9507 (CES2), 0.9453 (CDA), 0.9714 (TP), and 0.9947 (DPYD), with *P*-values of 0.0199, 0.0036, 0.0044, 0.0012, and < 0.0001, respectively. The strong correlation between the IHC staining index and PRM quantification results in both tumor and non-tumorous tissues indicates that the IHC staining index can accurately reflect the expression levels of each metabolic enzyme.

3.5 Risk factors affecting the expression of CAP metabolic enzymes in tumor tissue

This study employed Pearson correlation analysis to evaluate inter-tissue expression correlations of CAP-metabolizing enzymes, shown in a heatmap (Fig. 5). Only CES2 demonstrated a moderate positive correlation between tumor and non-tumorous tissues. Subsequent multivariate linear regression analyzed factors influencing HCC tissue enzyme expression across three domains: inter-enzyme interactions, pathological features, and clinical parameters. To optimize analytical rigor, LASSO regression screened all variables before modeling. Results of univariate and multivariate analyses are presented as forest plots (Figs. 6, 7, 8), with complete regression data available in Supplementary Tables 1–15.

Table 3 summarizes risk factors influencing CAP-metabolizing enzyme expression in HCC tissues. CES1 expression lacked identifiable risk factors, suggesting independence from other enzymes and clinicopathological variables. CES2 expression was associated with non-tumorous CES2 levels, histological grade, TS, P53, age, advanced CNLC (III-IV), T staging (T3-4), IBIL, and hydroperitoneum. For CDA, independent predictors included non-tumorous DPYD expression,

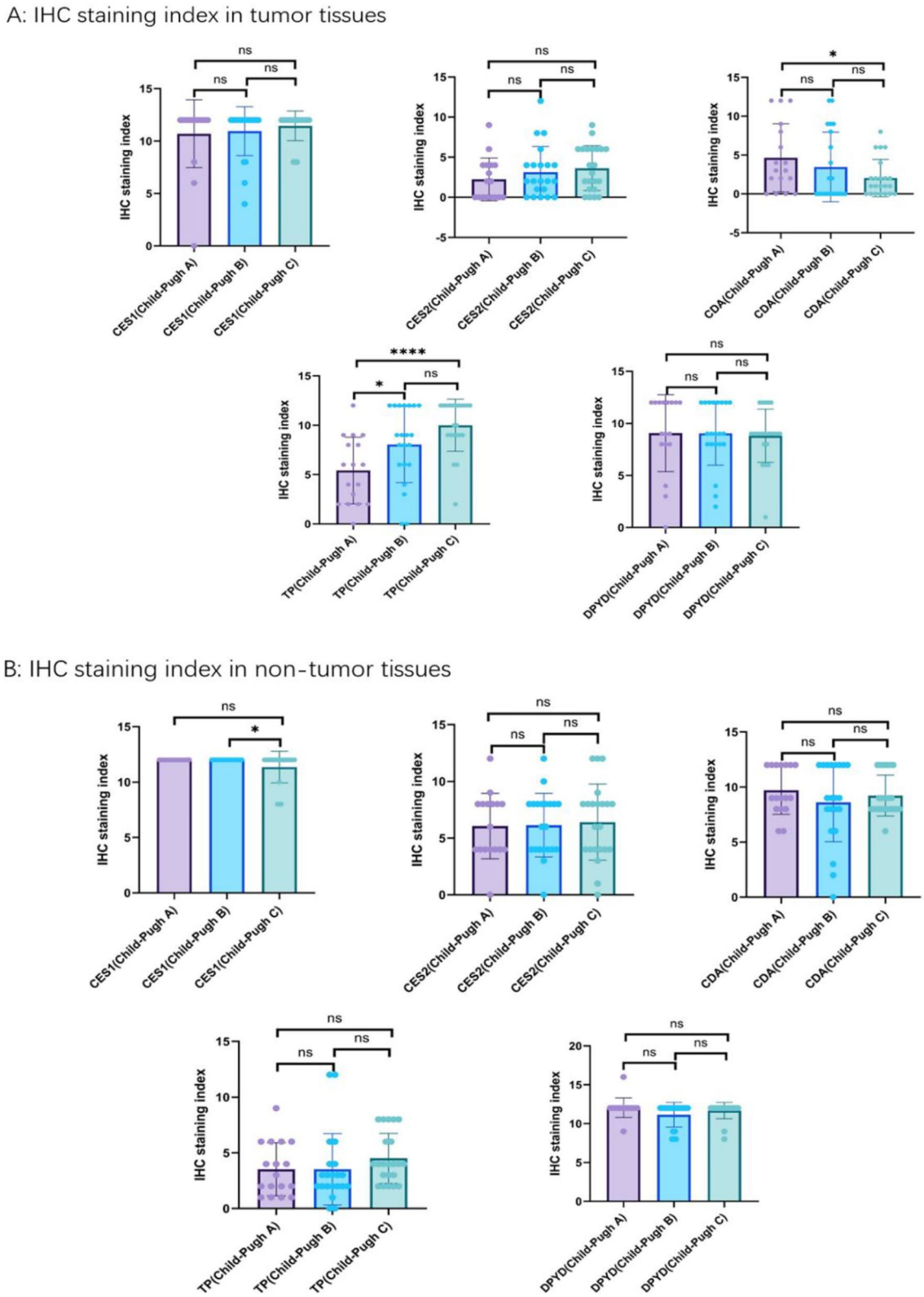

Fig. 2 Differential analysis of IHC staining index at different levels of liver function (**A** IHC staining index in HCC tumor tissues; **B** IHC staining index in non-tumor tissues; *ns* not significant, $P > 0.05$; * $P < 0.05$; **** $P < 0.01$)

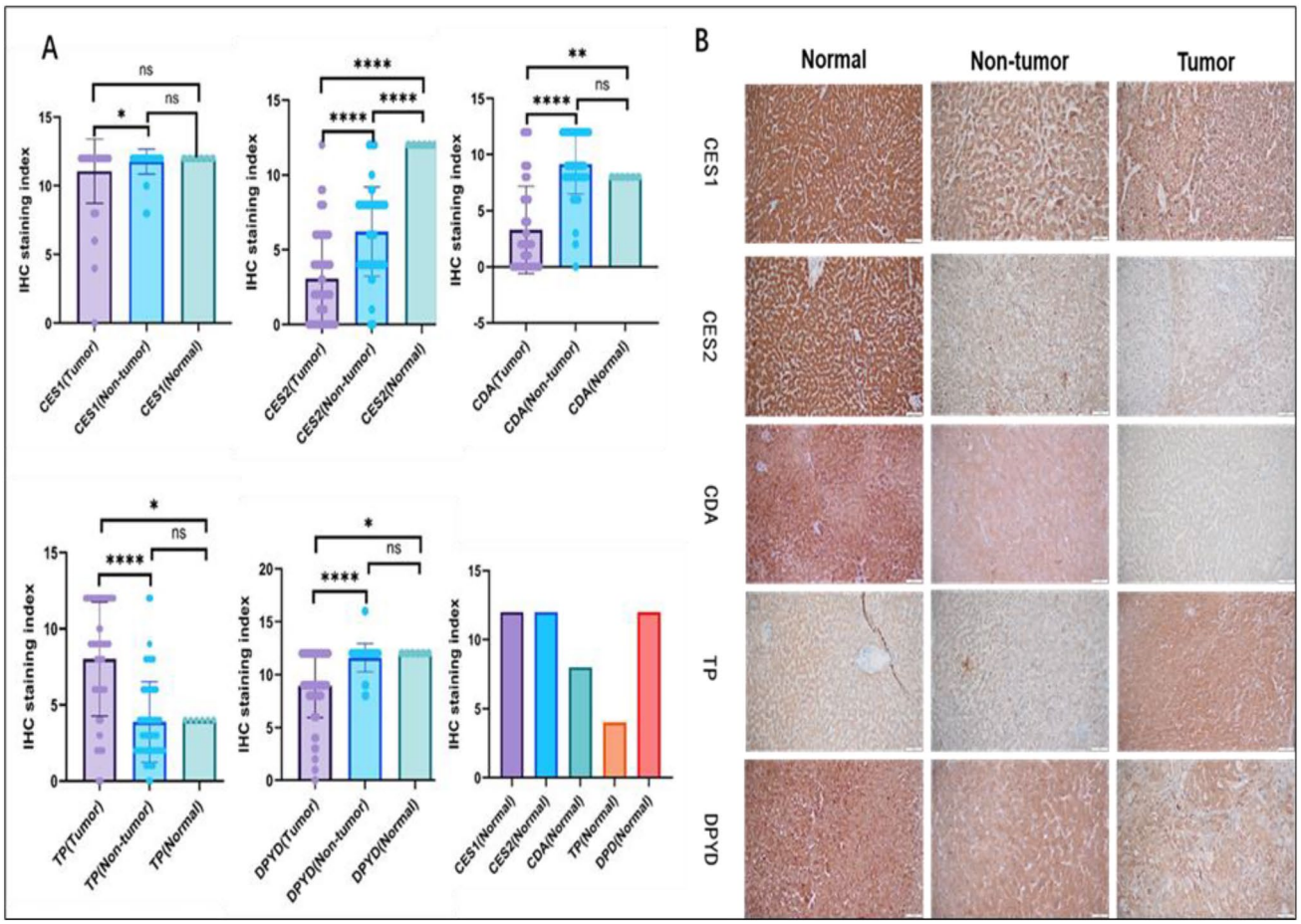

Fig. 3 Differential analysis of IHC staining index in different tissues (**A** IHC staining index in different tissues; **B** Analysis of the different tissues by IHC; *ns* not significant, $P > 0.05$; */** $P < 0.05$; **** $P < 0.01$)

Table 2 Discrete expression of capecitabine-related metabolizing enzymes in different tissues

CAP metabolizing enzyme[a]	Normal liver tissue (n = 6)		HCC tissue (n = 60)		Non-HCC tissue (n = 60)		*P* value[d]
	CV (%)[b]	Mean ± SD[c]	CV (%)	Mean ± SD	CV (%)	Mean ± SD	
CES1	0.000	12.00 ± 0.000	21.17	11.07 ± 2.342	7.724	11.77 ± 0.9088	**0.0330**
CES2	0.000	12.00 ± 0.000	94.90	3.067 ± 2.910	48.04	6.217 ± 2.986	**< 0.0001**
CDA	0.000	8.00 ± 0.000	118.7	3.283 ± 3.897	29.01	9.150 ± 2.654	**< 0.0001**
TP	0.000	4.00 ± 0.000	46.70	8.017 ± 3.744	68.23	3.883 ± 2.650	**< 0.0001**
DPYD	0.000	12.00 ± 0.000	33.80	8.967 ± 3.031	11.58	11.60 ± 1.343	**< 0.0001**

Bold values indicate statistically significant *P* values (< 0.05)

[a]IHC staining index

[b]CV: Coefficient of variation

[c]SD: Standard deviation

[d]Differential comparison of HCC tissue and non-HCC tissue

histological grade III, PS score, and IBIL. TP expression was linked to Ki-67 and ALT. Although univariate analysis identified no DPYD risk factors, multivariate analysis implicated non-tumorous CES2 as its sole independent risk factor.

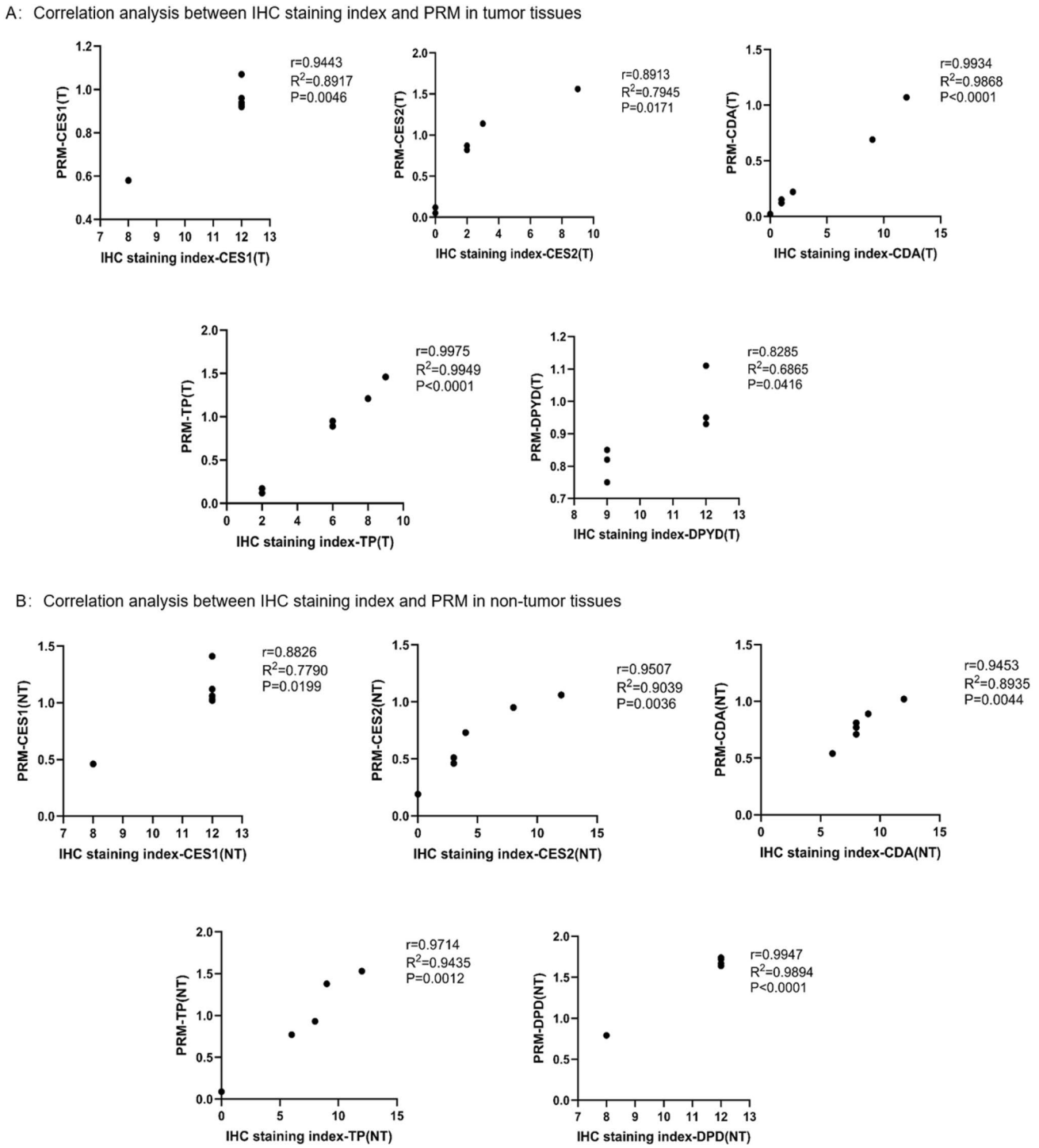

Fig. 4 Correlation analysis between IHC staining index and PRM (Parallel Reaction Monitoring) in different tissues (**A** Correlation analysis in tumor tissues; **B** Correlation analysis in non-tumor tissues)

3.6 Development of a treatment flowchart for CAP administration

Figure 9 outlines a treatment flowchart based on median IHC staining indices of CAP-metabolizing enzymes, designed to guide CAP therapy in HCC. The flowchart begins with assessing TP expression in tumors and CES1/CDA/DPYD in non-tumorous tissues. Negative results contraindicate CAP use. For positive cases, IHC indices are further stratified

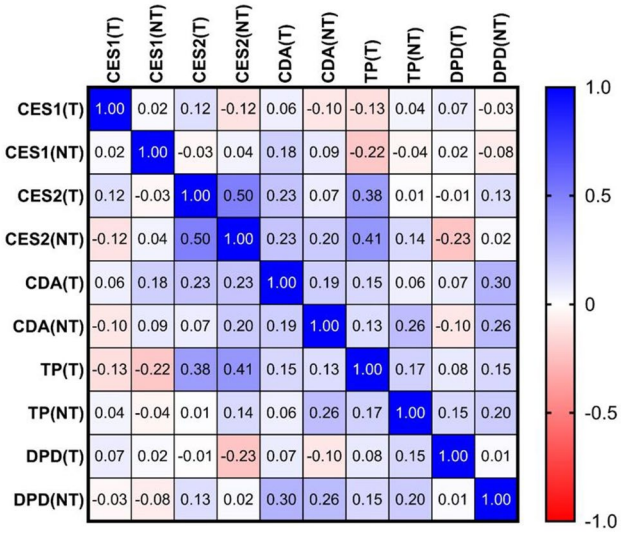

Fig. 5 Heatmap of correlations between CAP metabolic enzymes (T: Tumor; NT: non-tumor)

to assign treatment categories: ① CAP recommended (proven efficacy, minimal toxicity); ② CAP advised with liver function monitoring; ③ CAP with toxicity surveillance; ④ CAP cautiously administered (uncertain efficacy); ⑤ CAP contraindicated (poor efficacy/severe toxicity); ⑥ CAP excluded (no efficacy).

4 Discussion

The efficacy of CAP in treating HCC is not satisfactory, with positive efficacy only observed in advanced HCC patients [8]. Mechanistic studies addressing this limitation are scarce. The pharmacological activity of CAP is highly dependent on its metabolic conversion, which is strictly regulated by metabolic enzymes [14]. Given that most HCC patients have underlying liver disease, this study hypothesizes that the suboptimal efficacy of CAP may be linked to differences in the expression of metabolic enzymes. Consequently, this study systematically analyzed the expression heterogeneity of CAP metabolic enzymes in HCC patients and found significant individual and tissue differences, which were associated with clinical pathological factors such as liver function status and tumor differentiation. Based on these findings, this study successfully constructed a treatment flowchart for CAP application in HCC patients, providing a framework for personalized CAP treatment to optimize HCC treatment outcomes.

This study revealed a strong positive IHC-PRM correlation ($P < 0.05$), validating IHC as a reliable technology for quantifying CAP-metabolizing enzyme expression. Although the correlation analysis of DPYD detection by the two methods showed a P value of 0.0416 (approaching the significance threshold, $P < 0.05$), the correlation coefficient ($r = 0.8285$) indicated a strong positive correlation. This borderline significance may result from limited sample size or interindividual variability, and larger cohorts are warranted to improve statistical power in future research. However, this offers a precise and cost-effective detection method suitable for clinical application and ideal for large-scale screening. Moreover, this study systematically analyzes the correlation between CAP metabolic enzyme expression and liver function. In tumor tissue, CDA expression decreases with worsening liver function, whereas TP expression increases. Other metabolic enzymes are unaffected. No individual differences in metabolic enzyme expression were found in normal liver tissue, consistent with previous studies [7]. Existing studies suggest individual differences in CES1 and CES2 expression in normal liver tissue are influenced by genetic factors like single-nucleotide polymorphisms (SNPs) and non-genetic factors, including development, gender, and drug interactions [15, 16]. Although studies have suggested that the SNPs of CDA, TP, and DPYD may affect CAP metabolism and clinical effects [17, 18], direct evidence of individual differences in normal liver tissue is scarce. The study found significant individual differences in the expression of all metabolic enzymes in both tumor and non-tumorous tissues. In tumor tissue, individual differences in the expression of metabolic enzymes, except for TP, are more pronounced than in non-tumorous tissue, while TP exhibits an opposite trend. All samples in this study were from patients with HCC following hepatitis B and cirrhosis; thus, the non-tumorous tissue is cirrhotic. Therefore, HCC may amplify individual differences in metabolic enzymes other than TP. After HCC develops, however, TP's differences tend to decrease, which is consistent with previous studies [19].

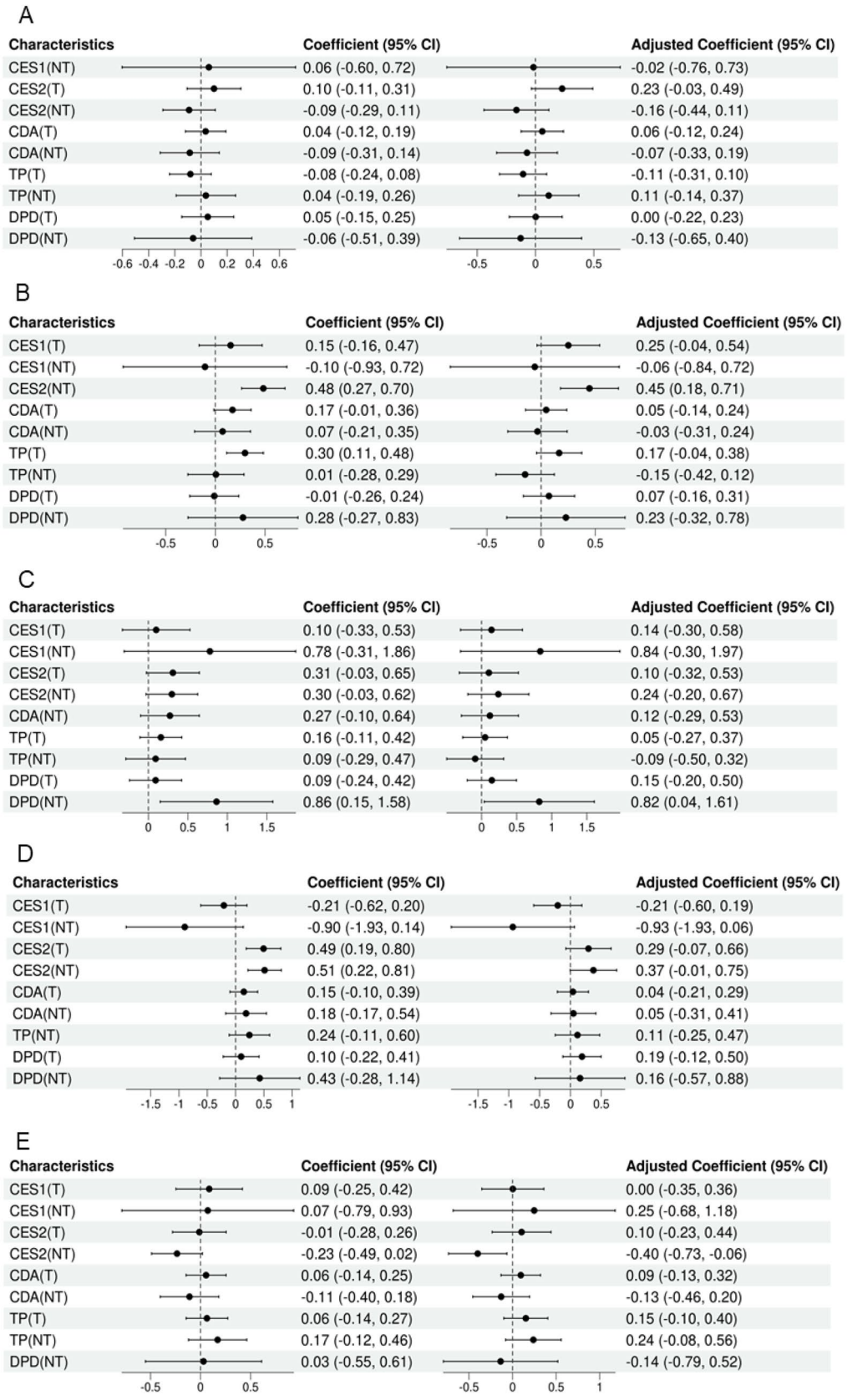

Fig. 6 The forest map of influencing factors between CAP metabolic enzymes in HCC tissue (Linear regression) (**A** CES1; **B** CES2; **C** CDA; **D** TP; **E** DPYD; T: Tumor; NT: Non-tumor)

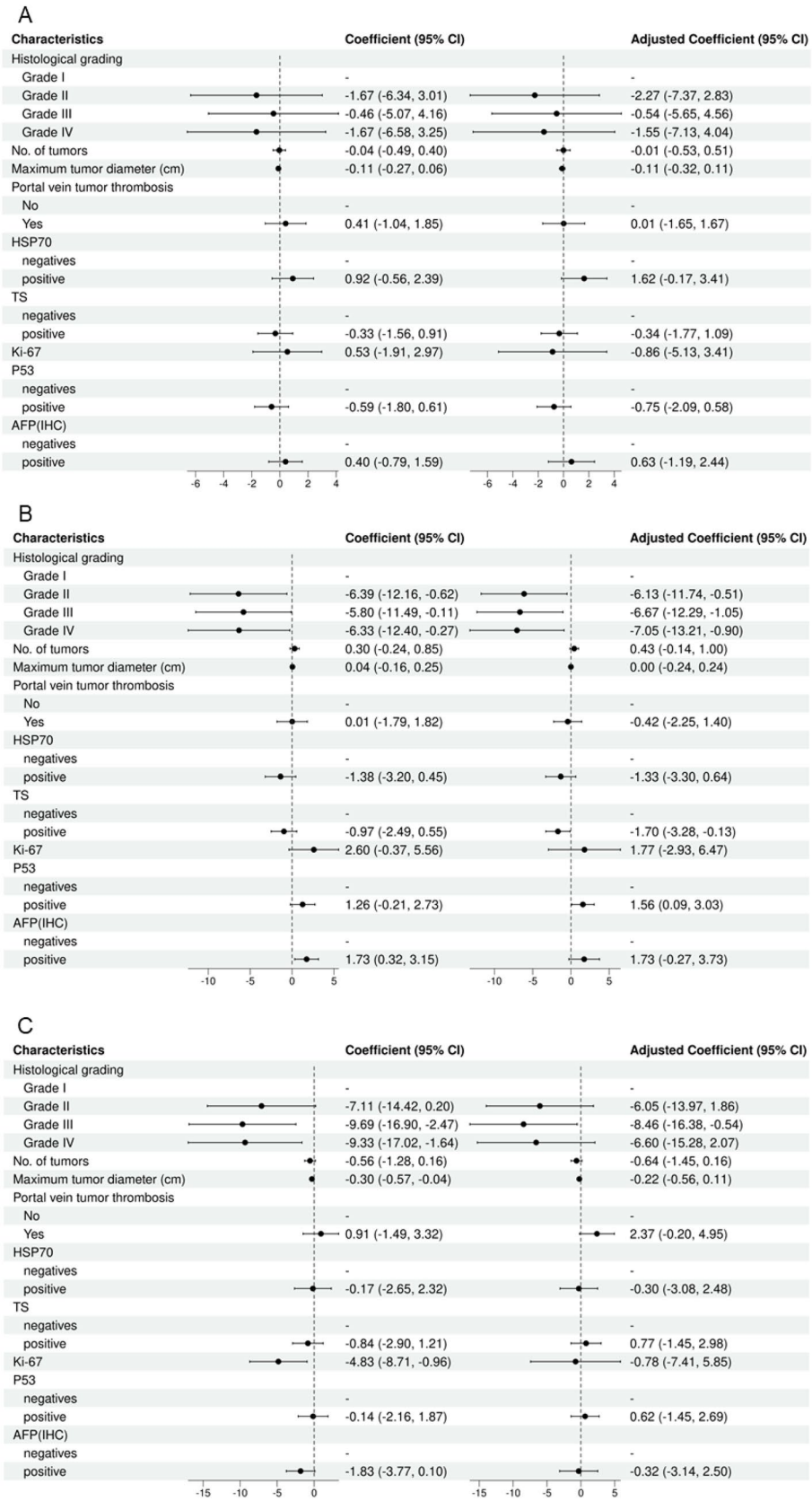

Fig. 7 The forest map of influencing factors between CAP metabolic enzymes and pathologic indicators in HCC tissue (linear regression) (**A** CES1; **B** CES2; **C** CDA; **D** TP; **E** DPYD)

Fig. 7 (continued)

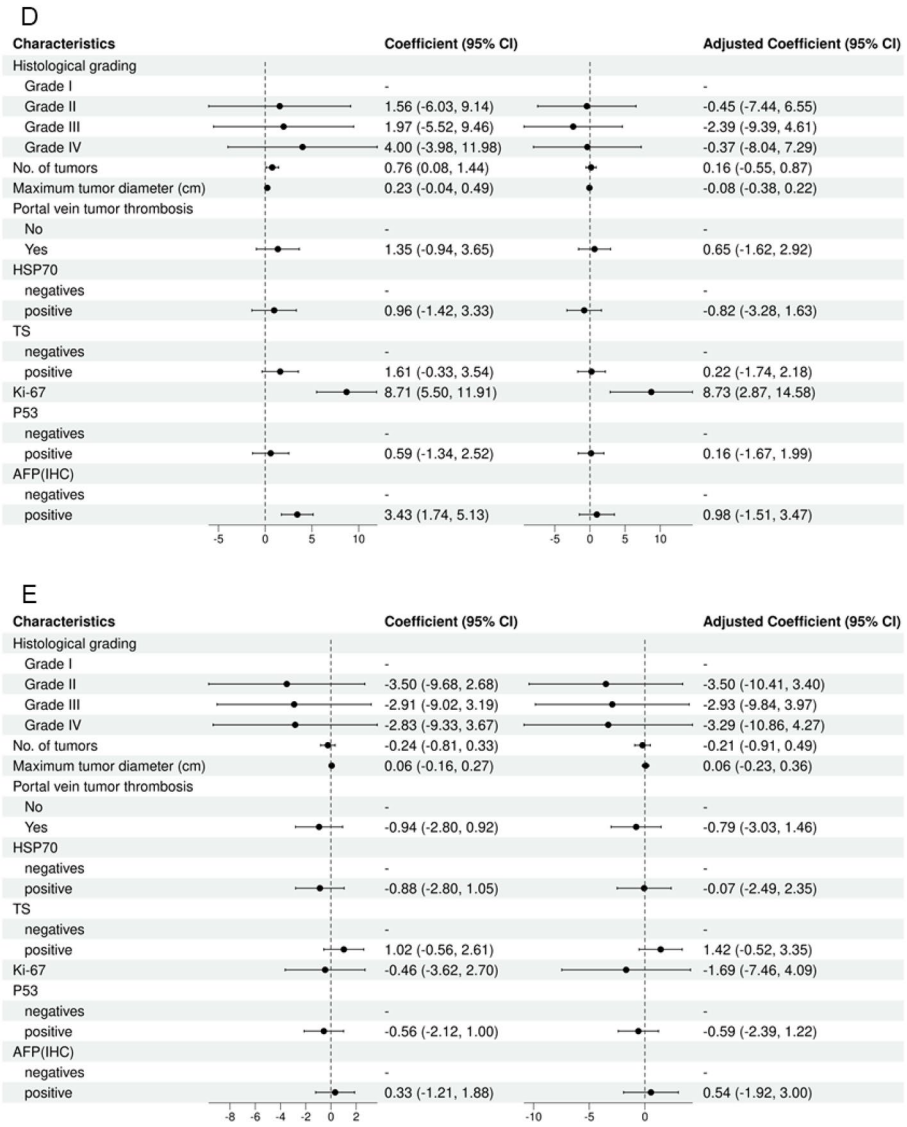

This study evaluated tissue-specific expression variability of CAP-metabolizing enzymes. The findings revealed that CES1 expression was marginally reduced in tumor tissue, with no significant difference from other tissues. A study by Li G et al. also noted that CES1 expression in liver cancer was lower than in normal liver, particularly in bile duct carcinoma [20]. This study observed a progressive decline in CES2 expression from normal liver to tumor tissue, hinting at a link between CES2 expression and tumor progression. High CES2 expression in pancreatic ductal adenocarcinoma (PDAC) has been associated with better overall survival [21]. The study detected significantly lower CDA and DPYD expressions in tumor tissue compared to non-tumorous and normal liver tissue. Previous research has indicated that diminished CDA expression in tumor cells may disrupt DNA stability and repair, fostering tumorigenesis [22]. CES2, CDA, and DPYD expression universally decrease with significant individual differences as tumors evolve. CES2 shows a gradual decline, while CDA and DPYD exhibit more abrupt changes. This suggests that alterations in these enzymes'expression may be tied to hepatocyte malignant transformation. In normal liver tissue, these enzymes likely play roles in maintaining liver physiology, including metabolism, detoxification, and cell proliferation. Their expressions may alter in response to liver pathologies such as chronic inflammation or cirrhosis. The significant reduction in these enzymes'expressions during liver cancer progression could be attributed to rapid tumor cell proliferation, metabolic irregularities, and microenvironmental shifts [23, 24]. Conversely, this study found that while TP exhibited the most significant individual differences in cirrhotic tissue, its expression in tumor tissue was markedly higher than in other tissues. This implies that TP expression might diverge before tumor onset, aligning with previous research. Zhang Q et al. also reported a substantial increase in TP in liver cancer tissue, with this upregulation closely associated with angiogenesis and prognosis in liver cancer tissue [25].

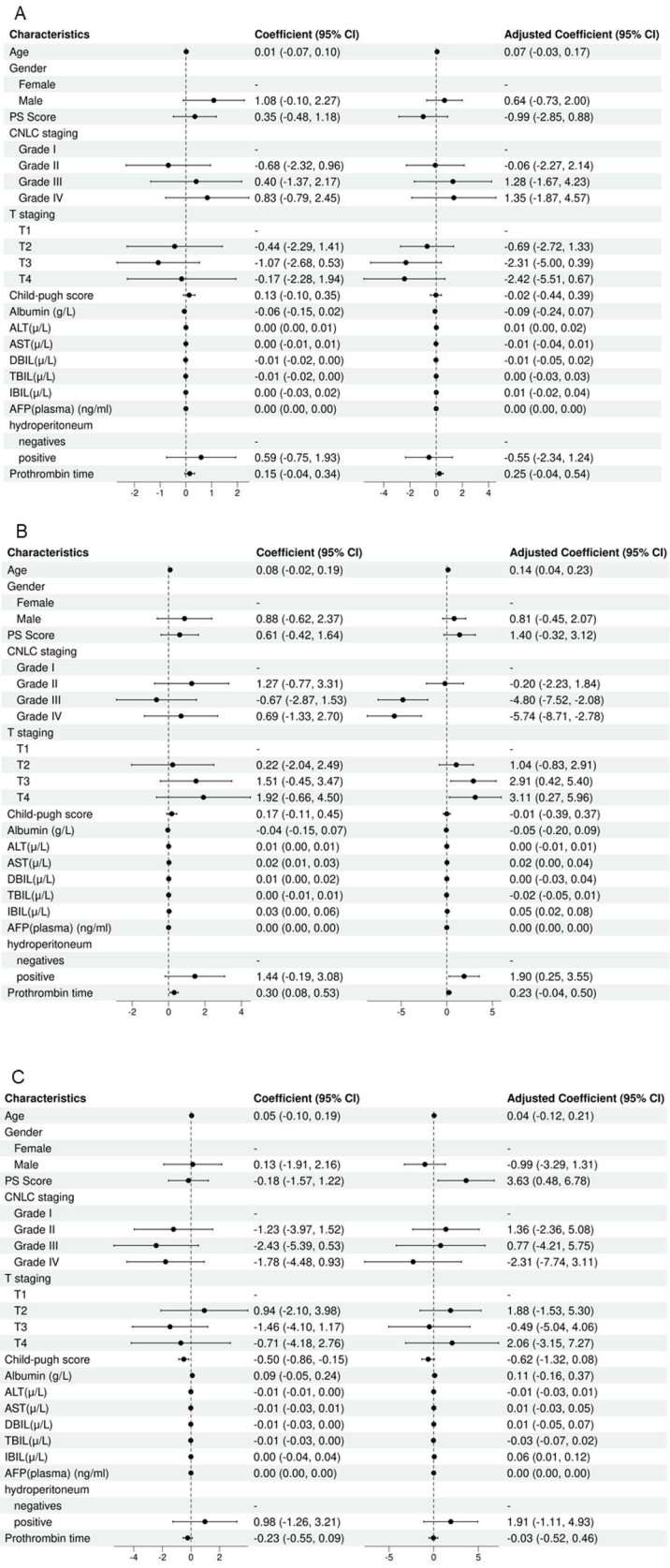

Fig. 8 The forest map of influencing factors between CAP metabolic enzymes and clinical indicators in HCC tissue (linear regression) (**A** CES1; **B** CES2; **C** CDA; **D** TP; **E** DPYD)

Fig. 8 (continued)

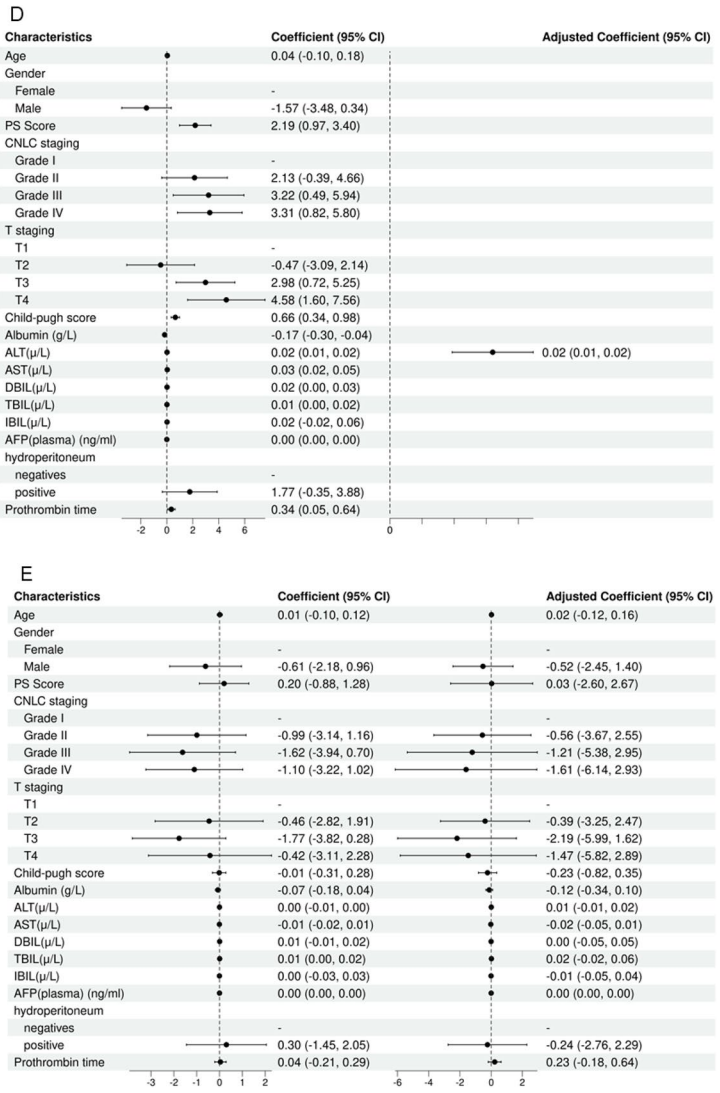

Among pro-angiogenic factors, TP and vascular endothelial growth factor (VEGF) play a crucial role in the promotion of angiogenesis in HCC tumors [26].

This study rigorously selected variables using LASSO regression and then employed linear regression to identify the risk factors affecting the expression of each metabolic enzyme. It was found that the expression of metabolic enzymes in tumor tissue is mutually independent. However, the expression of CES2 and DPYD in non-tumorous tissue serves as an independent risk factor for the expression of CES2, DPYD, and CDA in tumor tissue. This suggests that the heterogeneity of HCC tumors may be influenced by non-tumorous tissue, potentially at multiple levels including gene expression, metabolic changes, tumor microenvironment alterations, and non-traditional enzyme functions. Moreover, the expression of CES1 and DPYD in HCC tissue is independent of pathological and clinical factors, indicating that they are highly conserved and can be expressed across various tumors. Their expression appears to be uninfluenced by the tumor microenvironment, suggesting their potential as therapeutic targets. Conversely, this study determined that the expression of CES2, CDA, and TP in tumor tissue is influenced by multiple pathological and clinical factors, with CES2 and CDA being particularly sensitive. Pathological tissue grading emerges as an independent risk factor for their expression, indicating a close relationship with tumor differentiation. Additionally, P53 is identified as an independent risk factor for CES2 expression in tumor tissue, aligning with previous findings [27]. Notably, Ki-67 in tumor tissue is found to be an independent risk factor for TP expression, suggesting a close link between TP expression and tumor cell proliferation.

This study has the following innovative features and strengths: First, this study systematically investigated the expression differences of CAP metabolic enzymes across different tissues in HCC patients, emphasizing the importance of the metabolic enzyme cascade reaction and providing a basis for personalized CAP treatment. Second, this

Table 3 Risk factors and independent risk factors associated with CAP metabolizing enzyme expression in HCC tissues

CAP metabolic enzymes	Risk factors			Independent risk factors		
	Between metabolic enzymes	Pathological indicators	Clinical indicator	Between metabolic enzymes	Pathological indicators	Clinical indicator
CES1	None	None	None	None	None	None
CES2	CES2(NT) (95% CI 0.27, 0.70, $P < 0.001$) TP(T) (95% CI 0.11, 0.48, $P = 0.002$)	Histological grading: Grade II (95% CI − 12.16, − 0.62, $P = 0.034$); Grade IV (95% CI − 12.40, − 0.27, $P = 0.045$) AFP(IHC) (95% CI 0.32, 3.15, $P = 0.020$)	ALT (95% CI 0.00, 0.01, $P = 0.040$) AST (95% CI 0.01, 0.03, $P = 0.006$) Prothrombin time (95% CI 0.08, 0.53, $P = 0.011$)	CES2(NT) (95% CI 0.18, 0.71, $P = 0.002$)	Histological grading: Grade II (95% CI − 11.74, − 0.51, $P = 0.033$); Grade III (95% CI − 12.29, − 1.05, $P = 0.021$); Grade IV (95% CI − 13.21, − 0.90, $P = 0.026$) TS (95% CI − 3.28, − 0.13, $P = 0.034$) P53 (95% CI 0.09, 3.03, $P = 0.038$)	Age (95% CI 0.04, 0.23, $P = 0.004$) CNLC staging: Grade III (95% CI − 7.52, − 2.08, $P < 0.001$) Grade IV (95% CI − 8.71, − 2.78, $P < 0.001$) T staging: T3 (95% CI 0.42, 5.40, $P = 0.023$) T4 (95% CI 0.27, 5.96, $P = 0.033$) IBIL (95% CI 0.02, 0.08, $P = 0.002$) Hydroperitoneum (95% CI 0.25, 3.55, $P = 0.025$)
CDA	DPYD(NT) (95% CI 0.15, 1.58, $P = 0.021$)	Histological grading: Grade III (95% CI − 16.90, − 2.47, $P = 0.011$); Grade IV (95% CI − 17.02, − 1.64, $P = 0.021$) Maximum tumor diameter (95% CI − 0.57, − 0.04, $P = 0.029$); KI− 67 (95% CI − 8.71, − 0.96, $P = 0.018$)	Child–pugh score (95% CI − 0.86, − 0.15, $P = 0.007$)	DPYD(NT) (95% CI 0.04, 1.61, $P = 0.040$)	Histological grading: Grade III (95% CI − 16.38, − 0.54, $P = 0.037$);	PS Score (95% CI 0.48, 6.78, $P = 0.025$) IBIL (95% CI 0.01, 0.12, $P = 0.033$)

Table 3 (continued)

CAP metabolic enzymes	Risk factors			Independent risk factors		
	Between metabolic enzymes	Pathological indicators	Clinical indicator	Between metabolic enzymes	Pathological indicators	Clinical indicator
TP	CES2(T) (95% CI 0.19, 0.80, $P = 0.002$) CES2(NT) (95% CI 0.22, 0.81, $P = 0.001$)	No. of tumors (95% CI 0.08, 1.44, $P = 0.033$) KI– 67 (95% CI 5.50, 11.91, $P < 0.001$) AFP(IHC) (95% CI 1.74, 5.13, $P < 0.001$)	PS Score (95% CI 0.97, 3.40, $P < 0.001$) CNLC staging: Grade III (95% CI 0.49, 5.94, $P = 0.024$) T staging: T3 (95% CI 0.72, 5.25, $P = 0.013$) T4 (95% CI 1.60, 7.56, $P = 0.004$) Child–pugh score (95% CI 0.34, 0.98, $P < 0.001$) ALT (95% CI 0.01, 0.02, $P < 0.001$) AST (95% CI 0.02, 0.05, $P < 0.001$) DBIL (95% CI 0.00, 0.03, $P = 0.037$) Prothrombin time (95% CI 0.05, 0.64, $P = 0.026$)	None	KI– 67 (95% CI 2.87, 14.58, $P = 0.004$)	ALT (95% CI 0.01, 0.02, $p < 0.001$)
DPYD	None	None	None	CES2(NT) (95% CI − 0.73, − 0.06, $P = 0.020$)	None	None

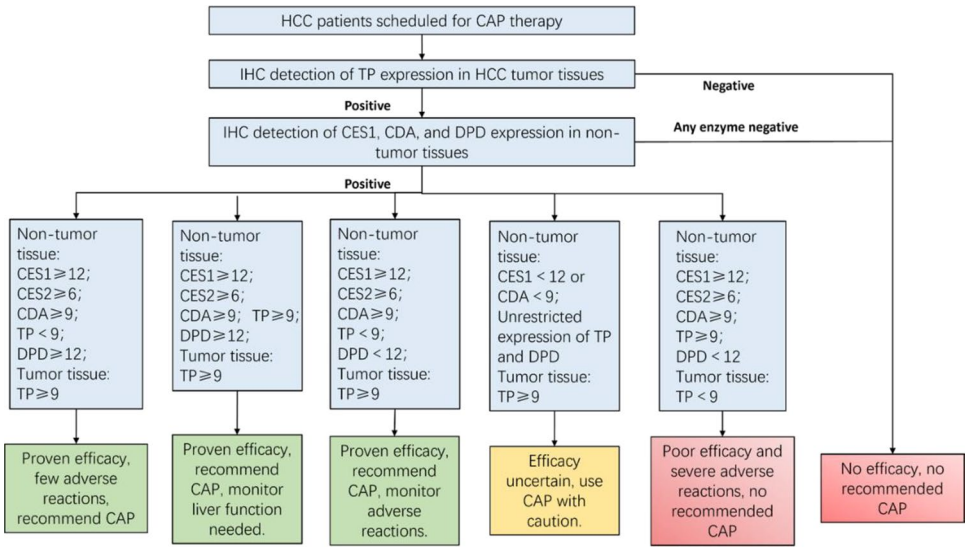

Fig. 9 Therapeutic flowchart of CAP application in HCC patients

study verified the accuracy of the IHC staining index using high-precision PRM protein quantification, enhancing its clinical application reliability. Third, this study used LASSO regression analysis to select variables and analyzed risk factors affecting CAP metabolic enzyme expression from multiple perspectives. Most notably, based on the IHC staining index, we developed a treatment flowchart for CAP application in HCC patients. This innovation aids personalized medicine implementation and provides a scientific basis for HCC treatment decisions, significantly enhancing the clinical value of this study.

This study has several limitations. First, its retrospective design introduces selection and information biases and lacks prospective randomized controlled trial validation. Future studies should use prospective designs and validate findings in diverse populations to enhance methodological rigor and generalizability. Secondly, the limited sample size (60 HCC patients, 6 normal controls) restricts the generalizability of the findings. Paired tumor/non-tumor tissues allowed for within-individual comparisons, but the small number of normal liver samples, due to donor scarcity, is insufficient to fully characterize baseline CAP metabolic enzyme expression. Future studies should expand cohort diversity through multicenter collaboration or alternative models to validate baseline CAP metabolic enzyme expression in normal liver tissue. Third, IHC and PRM provided robust protein quantification but did not assess enzymatic activity, an important determinant of metabolic function. Complementary approaches, such as fluorometric activity assays and CRISPR-based models, are needed to elucidate enzyme kinetics. Integrating multi-omics data (genomics, proteomics) could further unravel the molecular drivers of expression heterogeneity.

In summary, this study comprehensively analyzed the expression heterogeneity of CAP metabolic enzymes in HCC, which manifested as tissue and individual differences associated with liver function and clinical pathological factors. These findings suggest that such heterogeneity may contribute to the suboptimal efficacy of CAP in HCC. By developing a treatment workflow for CAP in HCC patients, this study underscores the importance of personalized metabolic enzyme analysis to enhance capecitabine efficacy and advance precision oncology.

Acknowledgements The authors extend our gratitude to Ms. Wenjuan Cai for her technical assistance in specimen acquisition and preliminary data curation.

Author contributions Conceptualization: HZ and Z-LW; Experimental operation: Z-QY, J-NL , J-LD , S-FC, and TC; Investigation and data curation: YZ, LC, and D-JK; Data curation and original draft preparation: JZ-QY and J-NL; Review: HZ and Z-LW. All authors have read and agreed to the submitted version of the manuscript.

Funding This study was supported by grants from the General Project of the Natural Science Foundation of Tianjin (22 JCYBJC01230).

Data availability Pathological samples were obtained from the institution's Biobank Resource Sharing Center. Clinical data and laboratory result data were collected through data collection forms from the hospital's computerized medical records. All data generated or analysed during this study are included in this published article and its supplementary information files. The datasets generated during and analysed during the current study are not publicly available due to individual privacy concerns, but are available from the corresponding author on reasonable request.

Declarations

Ethics approval and consent to participate This study adhered to the ethical principles of the Declaration of Helsinki and national regulatory standards, with formal approval granted by the Clinical Research Ethics Committee at Tianjin Medical University First Central Hospital (Approval ID: STEC-TFCH-2023-HM-2). Written informed consent was obtained from all participants or legal guardians before enrollment, explicitly authorizing the use of de-identified pathological specimens and clinical data for scientific investigation.

Consent for publication Not applicable.

Competing interests The authors declare no competing interests.

Human organ transplant statement Informed consent was obtained from all organ donors (or their legal guardians) and recipients. All organs used in the transplantation were legally and voluntarily donated, with explicit confirmation that no organs or tissues were sourced from prisoners. The study adhered to all relevant ethical and legal standards for human organ transplantation.

References

1. Tabata T, Katoh M, Tokudome S, Hosakawa M, Chiba K, Nakajima M, et al. Bioactivation of capecitabine in human liver: involvement of the cytosolic enzyme on 5'-deoxy-5-fluorocytidine formation. Drug Metab Dispos. 2004;32(7):762–7.
2. Alzahrani SM, Al Doghaither HA, Al-Ghafari AB, Pushparaj PN. 5-Fluorouracil and capecitabine therapies for the treatment of colorectal cancer (review). Oncol Rep. 2023;50(4):175.
3. Li Y, Zalzala M, Jadhav K, Xu Y, Kasumov T, Yin L, et al. Carboxylesterase 2 prevents liver steatosis by modulating lipolysis, endoplasmic reticulum stress, and lipogenesis and is regulated by hepatocyte nuclear factor 4 alpha in mice. Hepatology. 2016;63(6):1860–74.
4. Yasuno M, Mori T, Koike M, Takahashi K, Toi M, Takizawa T, et al. Importance of thymidine phosphorylase expression in tumor stroma as a prognostic factor in patients with advanced colorectal carcinoma. Oncol Rep. 2005;13(3):405–12.
5. Etienne-Grimaldi MC, Pallet N, Boige V, Ciccolini J, Chouchana L, Barin-Le Guellec C, et al. Current diagnostic and clinical issues of screening for dihydropyrimidine dehydrogenase deficiency. Eur J Cancer. 2023;181:3–17.
6. Lam SW, Guchelaar HJ, Boven E. The role of pharmacogenetics in capecitabine efficacy and toxicity. Cancer Treat Rev. 2016;50:9–22.
7. Wang Y, Hu H, Yu L, Zeng S. Physiologically based pharmacokinetic modeling for prediction of 5-FU Pharmacokinetics in cancer patients with hepatic impairment after 5-FU and capecitabine administration. Pharm Res. 2023;40(9):2177–94.
8. Pelizzaro F, Sammarco A, Dadduzio V, Pastorelli D, Giovanis P, Soldà C, et al. Capecitabine in advanced hepatocellular carcinoma: a multicenter experience. Dig Liver Dis. 2019;51(12):1713–9.
9. Mirestean CC, Iancu RI, Iancu DPT. Capecitabine-A "Permanent Mission" in head and neck cancers "War Council"? J Clin Med. 2022;11(19):5582.
10. Li J, Wang QB, Liang YB, Chen XM, Luo WL, Li YK, et al. Tumor-associated lymphatic vessel density is a reliable biomarker for prognosis of esophageal cancer after radical resection: a systemic review and meta-analysis. Front Immunol. 2024;15:1453482.
11. Mathew G, Agha R, Albrecht J, Goel P, Mukherjee I, Pai P, et al. STROCSS 2021: strengthening the reporting of cohort, cross-sectional and case-control studies in surgery. Int J Surg. 2021;96: 106165.
12. Zhang Q, Qin Y, Zhao J, Tang Y, Hu X, Zhong W, et al. Thymidine phosphorylase promotes malignant progression in hepatocellular carcinoma through pentose Warburg effect. Cell Death Dis. 2019;10(2):43.
13. Mullah MAS, Hanley JA, Benedetti A. LASSO type penalized spline regression for binary data. BMC Med Res Methodol. 2021;21(1):83.
14. Ge C, Huang X, Zhang S, Yuan M, Tan Z, Xu C, et al. In vitro co-culture systems of hepatic and intestinal cells for cellular pharmacokinetic and pharmacodynamic studies of capecitabine against colorectal cancer. Cancer Cell Int. 2023;23(1):14.
15. Liu Y, Li J, Zhu HJ. Regulation of carboxylesterases and its impact on pharmacokinetics and pharmacodynamics: an up-to-date review. Expert Opin Drug Metab Toxicol. 2024;20(5):377–97.
16. Xu M, Zhang L, Lin L, Qiang Z, Liu W, Yang J. Cisplatin increases carboxylesterases through increasing PXR mediated by the decrease of DEC1. J Biomed Res. 2023;37(6):431–47.
17. De With M, Van Doorn L, Maasland DC, Mulder TAM, Oomen-de Hoop E, Mostert B, et al. Capecitabine-induced hand-foot syndrome: a pharmacogenetic study beyond DPYD. Biomed Pharmacother. 2023;159: 114232.
18. Li J, Zhang W, Chen L, Mao X, Wang X, Liu J, et al. SNPs and blood inflammatory markers featured machine learning for predicting the efficacy of fluorouracil-based chemotherapy in colorectal cancer. Sci Rep. 2024;14(1):30635.
19. Du J, Zhang C, Liu F, Liu X, Wang D, Zhao D, et al. Distinctive metabolic remodeling in TYMP deficiency beyond mitochondrial dysfunction. J Mol Med (Berl). 2023;101(10):1237–53.
20. Li G, Li X, Mahmud I, Ysaguirre J, Fekry B, Wang S, et al. Interfering with lipid metabolism through targeting CES1 sensitizes hepatocellular carcinoma for chemotherapy. JCI Insight. 2023;8(2):e163624.

21. Kailass K, Casalena D, Jenane L, McEdwards G, Auld DS, Sadovski O, et al. Tight-binding small-molecule carboxylesterase 2 inhibitors reduce intracellular irinotecan activation. J Med Chem. 2024;67(3):2019–30.
22. Onclercq-Delic R, Buhagiar-Labarchède G, Leboucher S, Larcher T, Ledevin M, Machon C, et al. Cytidine deaminase deficiency in mice enhances genetic instability but limits the number of chemically induced colon tumors. Cancer Lett. 2023;555: 216030.
23. Kong D, Wang Z, Wang H, Yang R, Zhang W, Cao L, et al. Capecitabine mitigates cardiac allograft rejection via inhibition of TYMS-mediated Th1 differentiation in mice. Int Immunopharmacol. 2024;141: 112955.
24. Wang H, Yang R, Wang Z, Cao L, Kong D, Sun Q, et al. Metronomic capecitabine with rapamycin exerts an immunosuppressive effect by inducing ferroptosis of $CD4^+$ T cells after liver transplantation in rat. Int Immunopharmacol. 2023;124(Pt A): 110810.
25. Zhang Q, Zhang Y, Hu X, Qin Y, Zhong W, Meng J, et al. Thymidine phosphorylase promotes metastasis and serves as a marker of poor prognosis in hepatocellular carcinoma. Lab Invest. 2017;97(8):903–12.
26. Li J, Liang YB, Wang QB, Li YK, Chen XM, Luo WL, et al. Tumor-associated lymphatic vessel density is a postoperative prognostic biomarker of hepatobiliary cancers: a systematic review and meta-analysis. Front Immunol. 2025;15:1519999.
27. Qu W, Yao Y, Liu Y, Jo H, Zhang Q, Zhao H. Prognostic and immunological roles of CES2 in breast cancer and potential application of CES2-targeted fluorescent probe DDAB in breast surgery. Int J Gen Med. 2023;16:1567–80.